# Robust adaptive integral backstepping control of FC-SC-battery and traction motor based hybrid electric vehicles

Muhammad Muzammal Islam
*DEI - Politecnico di Bari*
Bari, Italy
muhammadmuzammal.islam@poliba.it

Sergio Bruno
*DEI - Politecnico di Bari*
Bari, Italy
sergio.bruno@poliba.it

Cosimo Iurlaro
*DEI - Politecnico di Bari*
Bari, Italy
cosimo.iurlaro@poliba.it

Massimo La Scala
*DEI - Politecnico di Bari*
Bari, Italy
massimo.lascala@poliba.it

***Abstract*—The shortage of fossil fuels, greenhouse gases impact on environment and the raising awareness in public about global warming issues shifted the focus of transport industry towards fuel cell hybrid electric vehicles. Furthermore, rough driving conditions like slippery highways, hilly areas and irregular terrains enhance the nonlinearities existing in vehicle models. Time varying parameters like resistance, capacitance, inductance and the nonlinearities can alter the performance efficiency of hybrid electric vehicles. In this paper, a robust adaptive integral backstepping controller has been proposed to attenuate the effects of parametric uncertainties while considering the nonlinearities of system model. Lyapunov stability theory has been used to ensure the global asymptotic stability of the system. A worldwide harmonized light vehicle testing procedure has been used to test the speed of vehicle. The proposed adaptive nonlinear controller has been simulated on MATLAB/Simulink. The comparison study of proposed adaptive nonlinear controller has been considered with the recently suggested nonlinear controllers in the literature. To ensure the effectiveness of proposed controller in real-time, a controller hardware in loop experimental test has been considered.**

***Index Terms*—Fuel cell hybrid electric vehicles, Lyapunov stability, robust adaptive integral backstepping controller, controller hardware in loop**

## I. Introduction

The entire world is facing some major problems like global warming, shortage of fossil fuel and periodically increasing prices of fuel, so these problems drawing the attentions of automotive industry towards the fuel efficient vehicles. Fuel cell hybrid electric vehicle provides optimum solutions of the conventional problems of electric vehicles. Fuel cell is the extensive source of green energy and provides good driving range with no carbon emission [1], [2].

In literature different types of hybrid vehicles are proposed such as, Battery Electric Vehicles (BEVs), Plug in Hybrid Electric Vehicles (PHEVs) and Fuel Cell Hybrid Electric Vehicles (FHEVs) with different power trains configurations [3]. In [4] a study on supercapacitor and fuel cell has been considered to regulate the output voltage of HEVs. Similarly, in [5] a study has been considered on the fusion of fuel cell, supercapacitor and battery.

In literature, different configurations of power converters have been suggested to maintain the best coupling between the different energy source which constitute a hybrid vehicle. A derived and integrated boost flyback converter has been proposed for the FHEVs [6], however, this configuration can be found computationally complex in design. A cascaded converter based on multiport is introduced for variable reluctance motor based HEVs [7]. In this case, results exhibited overshoots/undershoots during the switching phenomenon.

As shown in [8], the vehicle model is characterized by the presence of nonlinearities due to the action of friction forces. These forces can modify the load torque and cause a significant enhancement of vehicle nonlinear behaviour.

A robust nonlinear control for battery based electric vehicle charger is considered for grid to vehicle applications [9], without proposing any adaptive laws for attenuating the effects of time varying parameters. An adaptive terminal synergetic and adaptive synergetic based nonlinear controllers have been proposed in [10] for DC output voltage regulation of FHEV. However, these developed methods are computationally complex and exhibited overshoots/undershoots. In [11] a multistage adaptive nonlinear control algorithm has been considered for ultracapacitor and battery based plugin hybrid electric vehicles. The developed multistage algorithm is computationally complex.

Backstepping and synergetic controllers are developed for electric power stage of fuel cell vehicles [12]. These established controllers alone do not deal with the effects of time varying parametric uncertainties of system model due to the nonavailability of adaptive control mechanism. In [13], the authors demonstrated the feasibility of applying a sliding mode

978-88-87237-55-9 ©2022 AEIT

control algorithm, along with all its variants, to control the current outputs in a fuel cell, supercapacitor and battery FHEV. The proposed method worked well but exhibited the arising of chattering phenomenon.

More recently, the authors in [14] have proposed the use of nonlinear controllers for optimizing the combined response of energy sources in a hybrid electric vehicle. The two developed controllers, namely an Integral Backstepping Sliding Mode Controller (IBS+SMC) and a Backstepping Sliding Mode Controller (BS+SMC), have been proposed to control the voltage of the DC bus and for speed tracking of FHEV. These controllers do not possess the ability to attenuate the effects of time-varying parametric uncertainties of system model, simply because there is no adaptation mechanism is incorporated within the control algorithms. Furthermore, the speed of driving unit was tested by considering an older driving cycle known as European Extra Urban Driving Cycle (EUDC). The drift of system parameters may cause a degradation of driving performance and a reduction of the vehicle useful life.

For such reasons, in this paper, an Adaptive Integral Backstepping Sliding Mode Controller(AIBS+SMC) is proposed and a latest driving cycle namely Worldwide harmonized Light Vehicle Testing Procedure is considered for speed tracking of vehicle. This proposed controller (AIBS+SMC) has not only the ability to attenuate the effects of parametric uncertainties of system model, but also exhibits better robustness against external disturbances to improve the driving performance of vehicle. The main control objectives of this research study are:

- To efficiently attenuate the effects of parametric uncertainties of system model.
- An accurate DC bus voltage control according to the varying load demand.
- 3-phase induction motor speed should be correctly tracked when subjected to Worldwide harmonized Light Vehicle Testing Procedure (WLTP).
- Lyapunov asymptotic stability of the system should be guaranteed.
- To check the real-time performance of proposed controller.

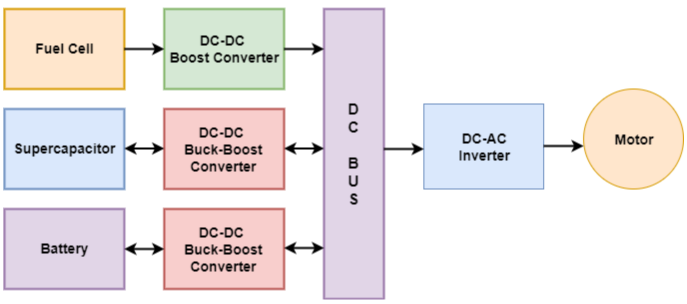


Fig. 1. Simplified scheme of a fuel cell, supercapacitor, battery FHEV

## II. Mathematical Modelling of FHEV Model

The FHEV configuration considered in this study can be schematized as in Fig 1. Three different energy sources (FC, SC and battery) are coupled to supply energy to an electric motor via the DC-bus. FC is used as main source of the power while SC is used to provide peak load acceleration demand for the short time interval. Battery is used to absorb the energy produce during regenerative braking to improve driving range of vehicle. Since the FC lacks the capability to store excessive amount of energy, either received from different energy resources or through braking control, a single directional DC-DC boost converter was applied to the FC.

The mathematical model that describes this system is given by the equations (1)-(9) [14]. The differential equations can easily be derived applying Kirchhoff laws to the equivalent electric circuit shown in Fig 2. The entire FHEV model is

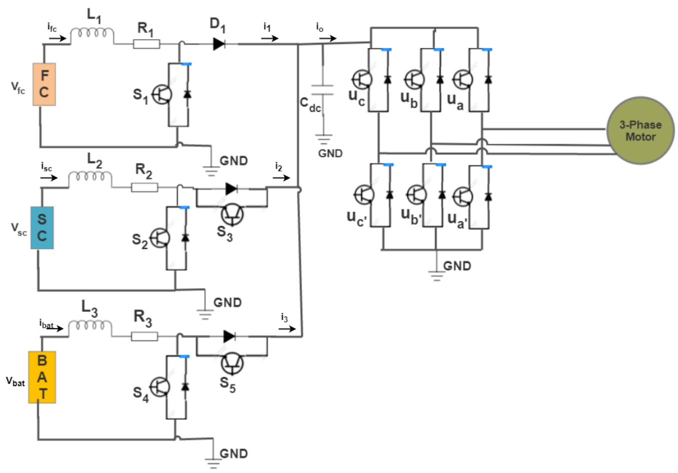


Fig. 2. Electric circuit diagram of FHEV

represented by differential equations as in [14],

$$\dot{x}_1 = -(1-u_1)\frac{x_4}{L_1} - \frac{R_1}{L_1}x_1 + \frac{v_{fc}}{L_1} \tag{1}$$

$$\dot{x}_2 = -u_{23}\frac{x_4}{L_2} - \frac{R_2}{L_2}x_2 + \frac{v_{uc}}{L_2} \tag{2}$$

$$\dot{x}_3 = -u_{45}\frac{x_4}{L_3} - \frac{R_3}{L_3}x_3 + \frac{v_{bat}}{L_3} \tag{3}$$

$$\dot{x}_4 = (1-u_1)\frac{x_1}{C_{dc}} + u_{23}\frac{x_2}{C_{dc}} + u_{45}\frac{x_3}{C_{dc}} - u_d\frac{x_5}{C_{dc}} - u_q\frac{x_6}{C_{dc}} \tag{4}$$

$$\dot{x}_5 = bax_7 + bpx_9x_8 - \gamma x_5 + \omega_s x_6 + m_1u_dx_4 \tag{5}$$

$$\dot{x}_6 = bax_8 - bpx_9x_7 - \gamma x_6 - \omega_s x_5 + m_1u_qx_4 \tag{6}$$

$$\dot{x}_7 = -ax_7 + (\omega_s - px_9)x_8 + aM_{sr}x_5 \tag{7}$$

$$\dot{x}_8 = -ax_8 - (\omega_s - px_6)x_7 + aM_{sr}x_6 \tag{8}$$

$$\dot{x}_9 = m(x_7x_6 - x_8x_5) - cx_9 - \frac{T_l}{J} \tag{9}$$

where $x_1$ to $x_3$ represent the mean values of the FC, supercapacitor and battery currents, respectively, $x_4$ is the DC bus voltage, whereas states $x_5$ and $x_6$ are the d-q axis rotating frame of the reference stator currents. Likewise, states $x_7$ and $x_8$ are the d-q axis rotating frame of reference rotor fluxes.

Finally, $x_9$ represents the angular speed of induction motor, based on three phases.

For the sake of reducing various effects of parametric uncertainties of system model the unknown parameters are adapted as, $\gamma_1 = \frac{1}{L_1}$, $\gamma_2 = \frac{1}{L_2}$, $\gamma_3 = \frac{1}{L_3}$, $\gamma_4 = \frac{R_1}{L_1}$, $\gamma_5 = \frac{R_2}{L_2}$, $\gamma_6 = \frac{R_3}{L_3}$ and $\gamma_7 = \frac{1}{C_{dc}}$. Simplified mathematical model of FHEV can be obtained by putting the values of unknown parameters $\gamma_1$, $\gamma_2$, $\gamma_3$, $\gamma_4$, $\gamma_5$, $\gamma_6$ and $\gamma_7$ into (1) to (4) respectively as following;

$$\dot{x}_1 = -(1-u_1)x_4\gamma_1 - x_1\gamma_4 + v_{fc}\gamma_1 \tag{10}$$

$$\dot{x}_2 = -u_{23}x_4\gamma_2 - x_2\gamma_5 + v_{uc}\gamma_2 \tag{11}$$

$$\dot{x}_3 = -u_{45}x_4\gamma_3 - x_3\gamma_6 + v_{bat}\gamma_3 \tag{12}$$

$$\dot{x}_4 = (1-u_1)x_1\gamma_7 + u_{23}x_2\gamma_7 + u_{45}x_3\gamma_7 - u_d x_5\gamma_7 - u_q x_6\gamma_7 \tag{13}$$

## III. Robust adaptive integral backstepping controller design procedure

For the sake of design an adaptive integral backstepping sliding mode controller (AIBS+SMC), the initial step is to introduce the tracking error $e_1$ as followings;

$$e_1 = x_1 - x_{1ref} \tag{14}$$

where $e_1$ is the error among FC current and its desire value $x_{1ref}$. Due to non-minimum phase nature of fuel cell the $x_{1ref}$ is derived from DC bus reference voltage as,

$$x_{1ref} = \theta\left(\frac{v_{dcref}i_o - v_{sc}i_{scref} - v_{bat}i_{batref}}{v_{fc}}\right) \tag{15}$$

where $\theta$ is the ideality factor and it shows the reactive components losses. Its value must be greater than 1. Taking time derivative of (14), we obtain:

$$\dot{e}_1 = \dot{x}_1 - \dot{x}_{1ref} \tag{16}$$

Now introducing $\tilde{\gamma}_i$, which is the error between estimated value $\hat{\gamma}_i$ and actual value $\gamma_i$ of adapted parameters, we have:

$$\tilde{\gamma}_i = \hat{\gamma}_i - \gamma_i \quad i = 1,2,3.... \tag{17}$$

By substituting the value of $\dot{x}_1$ from (10) into (16), we get:

$$\dot{e}_1 = -(1-u_1)x_4\hat{\gamma}_1 - x_1\hat{\gamma}_4 + v_{fc}\hat{\gamma}_1 - \dot{x}_{1ref} \tag{18}$$

In order to achieve the integral action, the integral term added into $e_1$ as:

$$\eta = e_1 + \rho \tag{19}$$

where $\rho$ is given as:

$$\rho = \int_0^t (x_1 - x_{1ref})dt \tag{20}$$

Since $e_1$ must converge to zero, the Lyapunov candidate function has been chosen as:

$$V_1 = \frac{1}{2}{e_1}^2 + \frac{\alpha}{2}\rho^2 \tag{21}$$

where $\alpha$ has a positive value. By considering time derivative of (21), putting the value of $\dot{e}_1$ from (18) into it, ensuring the negative definiteness condition and after some simplifications, we get virtual control as $\hat{\gamma}_1 x_4$ and is represented by $\beta$, we get:

$$\beta = \frac{c_1e_1 - x_1\hat{\gamma}_4 - v_{fc}\hat{\gamma}_1 + \dot{x}_{1ref} - \alpha\rho}{(1-u_1)} \tag{22}$$

Now consider error $e_2$ to make the system stable by considering $\hat{\gamma}_1 x_4$=$\beta$

$$e_2 = \hat{\gamma}_1 x_4 - \beta \tag{23}$$

By taking time derivative of (23) and by replacing the values of $\dot{x}_4$ and $\dot{\beta}$ into it, after simplifications we get,

$$\dot{e}_2 = (1-u_1)x_1\hat{\gamma}_7 + u_{23}x_2\hat{\gamma}_7 + u_{45}x_3\hat{\gamma}_7 - u_d x_5\hat{\gamma}_7 - u_q x_6\hat{\gamma}_7 - \dot{\beta} \tag{24}$$

Taking account of composite Lyapunov candidate function to guarantee the convergence of both $e_1$ and $e_2$ to zero, as:

$$V_{c_1} = V_1 + \frac{1}{2}{e_2}^2 \tag{25}$$

Taking time derivative of (25), then by replacing the value of $\dot{V}_1$ into it and after some simplifications, we get:

$$\dot{u}_1 = \frac{(1-u_1)}{\beta}\Big[c_2e_2 - (1-u_1)e_1 + (1-u_1)x_1\hat{\gamma}_7\hat{\gamma}_1 + u_{23}x_2\hat{\gamma}_7\hat{\gamma}_1 + u_{45}x_3\hat{\gamma}_7\hat{\gamma}_1 - u_d x_5\hat{\gamma}_7\hat{\gamma}_1 - u_q x_6\hat{\gamma}_7\hat{\gamma}_1 - \dot{\beta}\Big] \tag{26}$$

Control law $u_1$ guarantees the tracking of FC current and voltage of DC bus to their desire values $x_{1ref}$ and $x_{4ref}$ accurately. Now for the robustness of controller a sliding surface introduced as:

$$S = b_1e_1 + b_2e_2 \tag{27}$$

where $b_1$ and $b_2$ both are positive constants. Now add a switching term into adaptive integral backstepping control law $u_1$ to make its robust. The accumulative control law written as:

$$u_1 = \int_0^t \dot{u}_1 dt - k.Sign(S) \tag{28}$$

where $k$ is a positive constant and Sign(S) is the signum function. Now consider the errors $e_3$ and $e_4$ to track the reference values of supercapacitor and battery currents namely as $x_{2ref}$ and $x_{3ref}$ respectively:

$$e_3 = x_2 - x_{2ref} \tag{29}$$

$$e_4 = x_3 - x_{3ref} \tag{30}$$

Taking time derivatives of eqs. (29) and (30), putting the values of $\dot{x}_2$ and $\dot{x}_3$ from eqs. (11) and (12) into it and after some simplifications, we get:

$$u_{23} = \frac{1}{x_4\hat{\gamma}_2}\Big[c_3e_3 - x_2\hat{\gamma}_5 + v_{uc}\hat{\gamma}_2 - \dot{x}_{2ref}\Big] \tag{31}$$

$$u_{45} = \frac{1}{x_4\hat{\gamma}_3}\Big[c_4e_4 - x_3\hat{\gamma}_6 + v_{bat}\hat{\gamma}_3 - \dot{x}_{3ref}\Big] \tag{32}$$

where $u_{23}$ and $u_{45}$ are the required control laws to track the reference values of supercapacitor and battery currents. While

$c_3$ and $c_4$ are positive constants. In order to attenuate the effects of parametric uncertainties of system model consider an adaptive Lyapunov candidate function as;

$$V_c = \frac{1}{2}e_1^2 + \frac{1}{2}e_2^2 + \frac{1}{2}e_3^2 + \frac{1}{2}e_4^2 + \frac{1}{2\epsilon_1}\tilde{\gamma}_1^2 + \frac{1}{2\epsilon_2}\tilde{\gamma}_2^2 + \frac{1}{2\epsilon_3}\tilde{\gamma}_3^2 + \frac{1}{2\epsilon_4}\tilde{\gamma}_4^2 + \frac{1}{2\epsilon_5}\tilde{\gamma}_5^2 + \frac{1}{2\epsilon_6}\tilde{\gamma}_6^2 + \frac{1}{2\epsilon_7}\tilde{\gamma}_7^2 \quad (33)$$

Taking time derivative of (33) and substituting the values of $\dot{e}_1$, $\dot{e}_2$, $\dot{e}_3$ and $\dot{e}_4$ into it. After some simplifications we get the adaptive laws are designed as;

$$\dot{\hat{\gamma}}_1 = \epsilon_1 proj\Big(\hat{\gamma}_1, e_1(-(1-u_1)x_4) + (e_1 v_{fc})\Big) \quad (34)$$

$$\dot{\hat{\gamma}}_2 = \epsilon_2 proj\Big(\hat{\gamma}_2, -e_3((u_{23})x_4) + (e_3 v_{uc})\Big) \quad (35)$$

$$\dot{\hat{\gamma}}_3 = \epsilon_3 proj\Big(\hat{\gamma}_3, -e_4((u_{45})x_4) + (e_4 v_{bat})\Big) \quad (36)$$

$$\dot{\hat{\gamma}}_4 = \epsilon_4 proj\Big(\hat{\gamma}_4, -(e_1 x_1)\Big) \quad (37)$$

$$\dot{\hat{\gamma}}_5 = \epsilon_5 proj\Big(\hat{\gamma}_5, -(e_2 x_2)\Big) \quad (38)$$

$$\dot{\hat{\gamma}}_6 = \epsilon_6 proj\Big(\hat{\gamma}_6, -(e_3 x_3)\Big) \quad (39)$$

$$\dot{\hat{\gamma}}_7 = \epsilon_7 proj\Big(\hat{\gamma}_7, e_2((1-u_1)x_1) + (e_2 u_{23} x_2) + (e_2 u_{45} x_3) + (e_2 u_d x_5) + (e_2 u_q x_6)\Big) \quad (40)$$

Now for tracking the motor speed, rotor flux on d-axis side and to ensure the entire stability of traction motor, we consider some tracking errors $e_5$, $e_6$, $e_7$ and $e_8$. By taking time derivatives of these tracking errors and by putting values into them and after some simplifications we obtained the control laws as;

$$u_d = \frac{1}{m_1 x_4}\Big[ - c_{7e7} - bax_7 - \omega_s x_6 + \gamma x_5 + \dot{x}_{5d} - aM_{sr}e_5 \Big] \quad (41)$$

$$u_q = \frac{1}{m_1 x_4}\Big[ - c_{8e8} + bpx_7 x_9 + \omega_s x_5 + \gamma x_6 + \dot{x}_{6d} - mx_7 e_6 \Big] \quad (42)$$

where $u_d$ and $u_q$ are the required control laws to track the reference values of d-axis rotor flux and motor speed. While $c_5$, $c_6$, $c_7$, and $c_8$, are positive constants. After some simplifications, the derivative of composite Lyapunov candidate function achieved as,

$$\dot{V}_c = -c_1{e_1}^2 - c_2{e_2}^2 - c_3{e_3}^2 - c_4{e_4}^2 - c_5{e_5}^2 - c_6{e_6}^2 - c_7{e_7}^2 - c_8{e_8}^2 \leq 0 \quad (43)$$

Equation (43) shows that entire system is globally asymptotically stable system.

## IV. Simulation Results

The efficiency of proposed adaptive controller is tested on MATLAB/Simulink because this software is compatible for Power Hardware in the loop (PHIL) real-time setup too, installed at LabZERO, Politecnico di Bari, Italy. Furthermore, for tracking the speed of vehicle, the proposed controller was tested considering the Worldwide harmonized Light Vehicle Testing Procedure (WLTP) [15]. The specifications data of power converters, energy resources and the three-phase induction motor are mentioned in Table I [14]. Table II shows the design parameters values of the proposed controller, which were obtained by using genetic algorithm.

TABLE I
SPECIFICATIONS OF FHEV MODEL

| Specifications | Values |
|---|---|
| Fuel Cell | $34KW, 350V, 250A$ |
| Battery | $288\ Vdc$, $13.9Ah$, Li-ion |
| Supercapacitor | $2700F$, $205Vdc$ |
| Resistances $R_1$, $R_2$ and $R_3$ | $20m\Omega$, $25m\Omega$, $30m\Omega$ |
| Inductances $L_1$, $L_2$ and $L_3$ | $3.3mH$, $3.6mH$, $3.9mH$ |
| Output Capacitance ($C_{out}$) | $1.66mF$ |
| Motor Type | 3-Phase induction motor |
| Stator Inductance ($L_s$) | $0.142H$ |
| Stator Resistance ($R_s$) | $1.633\Omega$ |
| Rotor Inductance ($L_r$) | $0.076H$ |
| Rotor Resistance ($R_r$) | $0.93\Omega$ |
| Mutual Inductance ($M_{sr}$) | $0.099H$ |
| Nominal Flux | $1Wb$ |
| No of poles ($p$) | 2 |
| Interia ($J$) | 0.0111 |

TABLE II
PARAMETERS OF AIBS+SMC

| Parameters | Values |
|---|---|
| Gains of controller | $c_1$, $c_2$, $c_3$, $c_4$ 1, 0.8, 1.5, 7e$^3$<br>$c_5$, $c_6$, $c_7$, $c_8$, $\alpha$ 2.1, 2.1, 1.7e$^3$, 1.7e$^3$, 1e$^{-4}$ |
| Gains of sliding surface | $k$, $b_1$, $b_2$ 1e$^{-5}$, 3e$^4$, 3e$^4$ |
| Gains of adaptive laws | $\epsilon_1$, $\epsilon_2$, $\epsilon_3$ 1e$^{-6}$, 1e$^{-6}$, 1e$^{-6}$<br>$\epsilon_4$, $\epsilon_5$, $\epsilon_6$, $\epsilon_7$, 9e$^{-3}$, 9e$^{-3}$, 9e$^{-3}$, 6e$^{-3}$ |

### A. Driving Cycle

In this research work, the speed of the vehicle has been tested by considering a latest driving cycle namely as, Worldwide harmonized Light Vehicle Testing Procedure (WLTP). This speed tracking driving procedure is based on four different speed ranges, low range (WL-L) from (0-600 s), medium (WL-M) from (601-1000 s), high (WL-H) from (1001-1400 s) and extra high range (WL-EH) from (1401-1800 s) according to the speed of vehicle and this approach is most likely based on the real-time driving habits of the drivers. Fig.3 represents the standard WLTP driving cycle [15].

### B. Comparison study

This subsection aims to compare the proposed AIBS+SMC controller with the other ones previously presented in the literature, namely IBS+SMC and BS+SMC. In this research work, the comparison has been made by considering the simulation behaviour of the hybrid electric vehicle while following the WLTP speed testing procedure and the DC bus

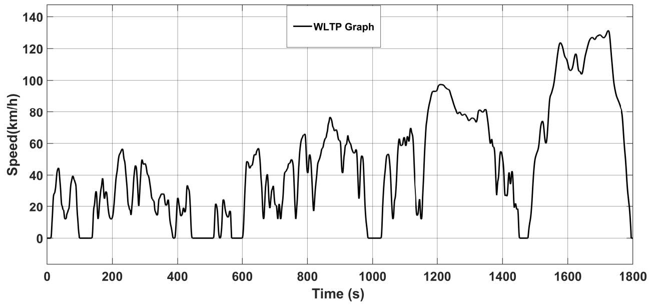


Fig. 3. WLTP driving cycle

voltage reference signal. From Fig. 4(a) it can be observed how some overshoots/undershoots appeared on the DC bus voltage signal in the various time intervals that are varied with the alternations of speed of the driving unit. These fluctuations were observed in all cases and were basically due to the changing effect of load current according to the load torque demand. Their magnitude level is lower in the case of the proposed AIBS+SMC controller.

From Fig. 4(b), it can be observed how the speed of FHEV is varied due to several gear shifts during the different time intervals and it is linked with the changing effect of DC bus voltage signal and load torque profile. So, overall the DC bus voltage and speed tracking of vehicle are achieved more efficiently in the case of AIBS+SMC as compared to IBS+SMC and BS+SMC controllers.

A numerical comparison of all the three controllers is given in Table III. This comparison is made while considering the WLTP driving cycle. The root mean square error (RMSE) of both DC-voltage and speed tracking of vehicle have been calculated for all the three controllers. In the case of AIBS+SMC controller, the RMSE value for the voltage tracking of DC bus is $0.7801$ while for the tracking of speed of motor is $0.0137$. The RMSE values of the DC voltage are sensibly higher in both IBS+SMC and BS+SMC cases (respectively $3.2378$ and $4.1613$). Also in the case of speed tracking, the RMSE values for IBS+SMC and BS+SMC are higher ($0.2201$ and $0.2587$, respectively). This comparison allows to conclude that, with respect to IBS+SMC and BS+SMC, the AIBS+SMC controller provides the better control performance by attenuating the effects of parametric uncertainties.

TABLE III
COMPARISON ANALYSIS ON THE BASIS OF RMSE

| Control techniques | Voltage control of DC bus (V) RMSE | Speed control (Km/h) RMSE |
|---|---|---|
| AIBS+SMC | 0.7801 | 0.0137 |
| IBS+SMC | 3.2378 | 0.2201 |
| BS+SMC | 4.1613 | 0.2587 |

## V. Controller Hardware in Loop Experimental Results

From section IV, it has been concluded that robust adaptive integral backstepping controller (AIBS+SMC) has not only attenuated the effects of time varying parameters of the system but also given the robust solution against external disturbances as compared to other proposed controllers in the literature.

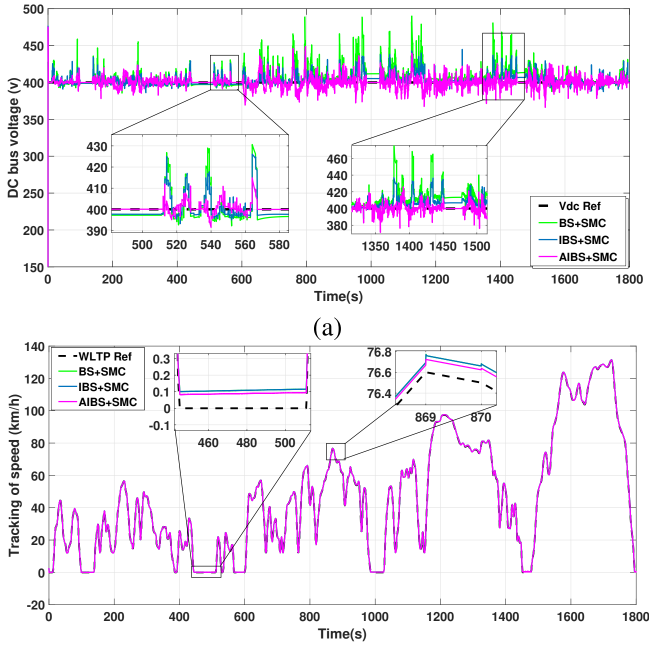


(a)

(b)

Fig. 4. Comparison analysis b/w AIBS+SMC, IBS+SMC and BS+SMC (a) DC-bus voltage tracking(b) speed tracking of vehicle

Now, in order to ensure the effectiveness of AIBS+SMC controller in real-time, a Controller Hardware-in-the-Loop (C-HIL) experimental test has been considered. Fig. 5 shows the C-HIL test bench setup used for obtaining real-time experimental results. For this purpose, C2000 Delfino$^{TM}$ along with two MCU F28379D launchpads, which are based on dual core CPU with an accumulative switching frequency of 20kHz, has been utilized.

The plant model is simulated on MATLAB/Simulink connected with launchpad 1 and the controller AIBS+SMC is implemented on launchpad 2 which has the switching frequency of 10kHz. Launchpad 2 then generates the duty ratios that are provided to launchpad 1 through PWM ports in the form of closed loop to to generate the real-time results. Fig. 6 represents the comparison between C-HIL based and simulations-based (same as proposed in the section IV-A) results in case of AIBS+SMC controller. From Fig. 6(a) and Fig. 6(b), it can be observed that, in case of C-HIL, both DC bus voltage and speed tracking signals showed some continuous fluctuations (as shown in the zoomed areas).

This behavior is due to the errors introduced in the control chain by the analog to digital conversion and by the communication system. However, the overall performance of AIBS+SMC in the real-time tests is up to the mark, in terms of both DC voltage and speed tracking of vehicle.

## VI. Conclusion

In this research paper, a robust adaptive integral backstepping controller has been proposed for tracking DC bus

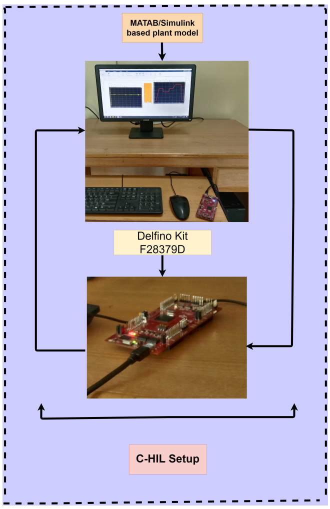


Fig. 5. Controller hardware in loop setup

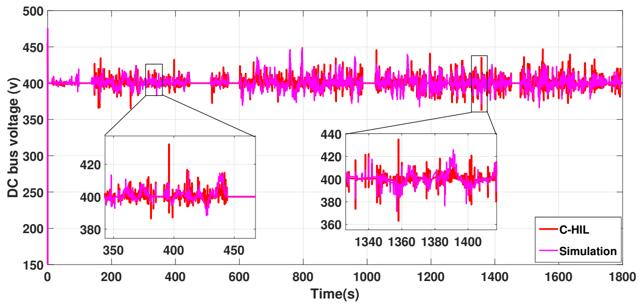


(a)

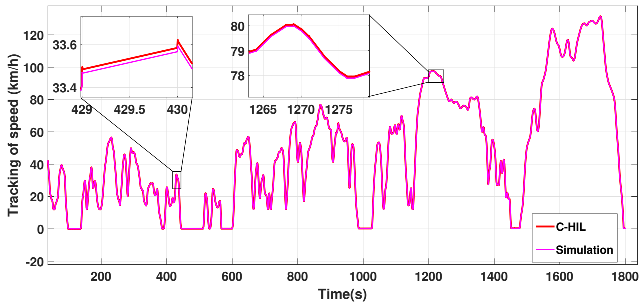


(b)

Fig. 6. C-HIL and simulation results comparison (a) Vdc tracking (b) Speed tracking

voltage control and speed tracking of a hybrid electric vehicle powered by fuel cell, supercapacitor and battery. The proposed robust adaptive nonlinear controller attenuated the effects of parametric uncertainties of system model. The performance efficiency of proposed nonlinear controller has been checked on MATLAB/Simulink. Comparative analysis of proposed nonlinear controller is considered with the suggested nonlinear controllers in the literature. Simulation results show that AIBS+SMC provides better robustness and control performance as compared to other controllers and it shows the better speed tracking of vehicle when it subjected to worldwide harmonized light vehicle testing procedure. A real-time Controller Hardware-in-the-Loop experimental test is considered to check the real-time performance of proposed controller. Future work may surround the implementation of proposed controller on real scenario by considering different converters and energy sources combinations to further improve the driving efficiency of vehicle.

## Acknowledgment

We acknowledge that Next Intelligence Research (NIR srl) company (website: https://www.next-tape.com/en/) is providing the scholarships to Mr. Muhammad Muzammal Islam and Mr. Cosimo Iurlaro for their PhD degrees research activities.

## References

[1] X. Lü, Y. Wu, J. Lian, Y. Zhang, C. Chen, P. Wang, and L. Meng, "Energy management of hybrid electric vehicles: A review of energy optimization of fuel cell hybrid power system based on genetic algorithm," *Energy Conversion and Management*, vol. 205, p. 112474, 2020.

[2] H. Sun, Z. Fu, F. Tao, L. Zhu, and P. Si, "Data-driven reinforcement-learning-based hierarchical energy management strategy for fuel cell/battery/ultracapacitor hybrid electric vehicles," *Journal of Power Sources*, vol. 455, p. 227964, 2020.

[3] M. Sabri, K. A. Danapalasingam, and M. F. Rahmat, "A review on hybrid electric vehicles architecture and energy management strategies," *Renewable and Sustainable Energy Reviews*, vol. 53, pp. 1433–1442, 2016.

[4] M. S. Khan, I. Ahmad, and F. Z. U. Abideen, "Output voltage regulation of fc-uc based hybrid electric vehicle using integral backstepping control," *IEEE Access*, vol. 7, pp. 65 693–65 702, 2019.

[5] H. Armghan, I. Ahmad, N. Ali, M. F. Munir, S. Khan, and A. Armghan, "Nonlinear controller analysis of fuel cell–battery–ultracapacitor-based hybrid energy storage systems in electric vehicles," *Arabian Journal for Science and Engineering*, vol. 43, no. 6, pp. 3123–3133, 2018.

[6] K.-C. Tseng, J.-T. Lin, and C.-A. Cheng, "An integrated derived boost-flyback converter for fuel cell hybrid electric vehicles," in *2013 1st International Future Energy Electronics Conference (IFEEC)*. IEEE, 2013, pp. 283–287.

[7] Q. Sun, J. Wu, C. Gan, J. Si, J. Guo, and Y. Hu, "Cascaded multiport converter for srm-based hybrid electrical vehicle applications," *IEEE Transactions on Power Electronics*, vol. 34, no. 12, pp. 11 940–11 951, 2019.

[8] M. G. Villella, "Nonlinear modeling and control of automobiles with dynamic wheel-road friction and wheel torque inputs," Ph.D. dissertation, Georgia Institute of Technology, 2004.

[9] I. Ahmed, I. Ahmad, S. Ahmed, and H. M. M. Adil, "Robust nonlinear control of battery electric vehicle charger in grid to vehicle applications," *Journal of Energy Storage*, vol. 42, p. 103039, 2021.

[10] M. M. Islam, S. A. Siffat, I. Ahmad, M. Liaquat, and S. A. Khan, "Adaptive nonlinear control of unified model of fuel cell, battery, ultracapacitor and induction motor based hybrid electric vehicles," *IEEE Access*, vol. 9, pp. 57 486–57 509, 2021.

[11] M. K. Azeem, H. Armghan, I. Ahmad, M. Hassan *et al.*, "Multistage adaptive nonlinear control of battery-ultracapacitor based plugin hybrid electric vehicles," *Journal of Energy Storage*, vol. 32, p. 101813, 2020.

[12] M. F. Munir, I. Ahmad, S. A. Siffat, M. A. Qureshi, H. Armghan, and N. Ali, "Non-linear control for electric power stage of fuel cell vehicles," *ISA transactions*, vol. 102, pp. 117–134, 2020.

[13] A. U. Rahman, I. Ahmad, and A. S. Malik, "Variable structure-based control of fuel cell-supercapacitor-battery based hybrid electric vehicle," *Journal of Energy Storage*, vol. 29, p. 101365, 2020.

[14] S. A. Siffat, I. Ahmad, A. U. Rahman, and Y. Islam, "Robust integral backstepping control for unified model of hybrid electric vehicles," *IEEE Access*, vol. 8, pp. 49 038–49 052, 2020.

[15] "Transport Policy, worldwide harmonized light vehicle testing procedure," https://www.transportpolicy.net/standard/international-light-duty-worldwide-harmonized-light-vehicles-test-procedure note = published: 2017.